Role of Specificity Protein-1 and Activating Protein-2 Transcription Factors in the Regulation of the Gap Junction Protein Beta-2 Gene in the Epididymis of the Rat[1]

Cécile Adam and Daniel G. Cyr[2]

Laboratory for Reproductive Toxicology, INRS-Institut Armand-Frappier, Université du Québec, Laval, Québec, Canada

ABSTRACT

In prepubertal rats, connexin 26 (GJB2) is expressed between adjacent columnar cells of the epididymis. At 28 days of age, when columnar cells differentiate into adult epithelial cell types, *Gjb2* mRNA levels decrease to barely detectable levels. There is no information on the regulation of GJB2 in the epididymis. The present study characterized regulation of the *Gjb2* gene promoter in the epididymis. A single transcription start site at position −3829 bp relative to the ATG was identified. Computational analysis revealed several TFAP2A, SP1, and KLF4 putative binding sites. A 1.5-kb fragment of the *Gjb2* promoter was cloned into a vector containing a luciferase reporter gene. Transfection of the construct into immortalized rat caput epididymal (RCE-1) cells indicated that the promoter contained sufficient information to drive expression of the reporter gene. Deletion constructs showed that the basal activity of the promoter resides in the first −230 bp of the transcriptional start site. Two response elements necessary for GJB2 expression were identified: an overlapping TFAP2A/SP1 site (−136 to −126 bp) and an SP1 site (−50 bp). Chromatin immunoprecipitation (ChIP) and electrophoretic mobility shift assays confirmed that SP1 and TFAP2A were bound to the promoter. ChIP analysis of chromatin from young and pubertal rats indicated that TFAP2A and SP1 binding decreased with age. SP1 and TFAP2A knockdown indicated that SP1 is necessary for *Gjb2* expression. DNA methylation did not appear to be involved in the regulation of *Gjb2* expression. Results indicate that SP1 and TFAP2A regulate *Gjb2* promoter activity during epididymal differentiation in rat.

developmental regulation, epididymal RCE cells, gene expression, SP1, TFAP2A, transcription factor

INTRODUCTION

Sperm maturation in the epididymis is critical for the acquisition of progressive motility and fecundity [1, 2]. Mammalian epididymis is composed of different regions or segments (initial segment, caput, corpus, and cauda), which have different morphological characteristics as well as different physiological functions [3]. At birth, epithelial cells of rat epididymis are undifferentiated [4, 5]. Cells are characterized by the absence of microvilli, few endocytic vesicles, and few secretory vesicles in the Golgi saccules [4]. Undifferentiated columnar cells begin to differentiate by Day 16 and differentiate into principal and clear cells by Day 28 [6]. Basal cells, which are also derived from columnar cells [4], first appear in the cauda region of the epididymis at Day 21 and are present throughout the epididymis by Day 28. The tight junctions of the blood-epididymis barrier begin forming during embryonic development and continue until Day 21 [7]. In mink, the barrier is impermeable at birth [8], but the timing of this occurrence in the rat is controversial [7, 9].

Connexins (Cxs) are a family of transmembrane proteins involved in intercellular gap junctional communication. Six Cxs form hexameric hemichannels, termed connexons, at the plasma membrane [10]. A transmembrane channel between two cells is formed when a connexon from one cell docks with a connexon of an adjacent cell. The agglomeration of transmembrane channels forms a gap junction between cells. Gap junctions allow cells to communicate by direct exchange of ions and small molecules (<1 kDa) [11]. Cxs provide selectivity to the transmembrane channel, and depending on the type(s) of Cxs that comprise the gap junction, the selectivity to certain ions or molecules that can pass through the transmembrane pores can change [12]. Gap junctional intercellular communication mediates important cellular processes including proliferation and differentiation of epithelia [13–17].

Gap junctions have been identified in epithelium of the epididymis [8, 18, 19] and appear to be crucial for maintaining cellular coordination along the epididymis and thus sperm maturation [19–22]. GJA1 (Cx43) was the first Cx identified in adult rat epididymis and is localized between principal and basal cells, as well as in the smooth muscle layer of the cauda epididymis [23]. Transgenic mice in which Cx43 has been mutated are subfertile and show altered sperm motility parameters [22]. In addition to GJA1, transcripts for *Gjb1* (Cx32), *Gjb2* (Cx26), *Gjb5* (Cx30.3), and *Gjb4* (Cx31.1) have also been identified in the epididymis [24]. Many of these connexins (GJA1, GJB4, and GJB5) have recently been reported to be expressed in basal cells of the epididymis, suggesting extensive basal cell-principal cell intercellular communication [25]. During postnatal epididymal differentiation there is a switch in the expression of Cxs [24]. In the proximal region of the epididymis, GJB2 is expressed primarily in young animals, when the epithelium is undifferentiated and is located between adjacent epithelial columnar cells that line the lumen of the epididymis. *Gjb2* mRNA levels decrease dramatically between Day 28 and 35 [24]. As *Gjb2* mRNA levels decrease, there is a concomitant increase in *Gjb4*, *Gjb5*, and *Gjb1* mRNA levels. *Gja1* mRNA levels, like those of *Gjb2*, are high early in postnatal development and begin to

decrease at Day 35 but remain detectable throughout adulthood.

The switch in expression of different Cxs indicates a modification in the gap junction intercellular communication between differentiating cells of the epididymis; this suggests a role for Cxs in differentiation of epithelium. It has been reported that during keratinocyte differentiation, expression levels of GJB2 and GJA1 decrease, whereas expression of GJB4 and GJB5 increase. This change is associated with changes in gap junctional permeability [26]. During cardiomyocyte differentiation of mouse embryonic stem cells, GJA5 (Cx40) is undetectable in undifferentiated cells, and transcript levels increase with the appearance of beating cells [27]. In the mouse mammary gland, GJB2 levels increase during pregnancy, whereas GJB1 is expressed only during lactation [28]. These data corroborate the notion of Cxs as being implicated in epithelial differentiation.

There is limited information regarding the transcriptional regulation of GJB2 in normal tissue. Studies in both mammary and endometrial epithelial cells have reported that *Gjb2* was up-regulated by activating protein 2 (TFAP2A) and specificity protein 1 (SP1) transcription factors [29–32], thereby indicating the importance of GC and GT boxes in the promoter of *Gjb2*. In the epidermis, GJB2 is down-regulated by Kruppel-like factor 4 (KLF4) transcription factor during acquisition of the epidermal barrier [16]. Mice lacking KLF4 display an overexpression of GJB2 in keratinocytes and have an impaired epidermal barrier. The role of KLF4 in the regulation of *Gjb2* has been questioned, as in human airway epithelial cells, KLF4 silencing has no effect on *Gjb2* mRNA levels [13].

In a variety of cancer cells, *Gjb2* is considered a tumor suppressor gene and, if overexpressed, can decrease cell proliferation [33–35]. In endometrial [36], lung [37, 38], and breast cancer cells [39], *Gjb2* is down-regulated as a result of hypermethylation of the *Gjb2* promoter.

There is no information on the mechanism(s) that regulates *Gjb2* transcriptional expression in the epididymis. However, decreased *Gjb2* mRNA and protein levels during epithelial differentiation suggest that GJB2 may play a role in differentiation of this tissue. As such, understanding the regulation of *Gjb2* may provide critical information regarding the factors implicated in the regulation of epididymal differentiation. The objective of this study was to elucidate the mechanism regulating the *Gjb2* gene in rat epididymis by characterizing the regulation of its gene promoter region.

MATERIALS AND METHODS

Animals

Prepubertal (25 days of age) and pubertal (42 days of age) male Sprague-Dawley rats were purchased from Charles River Laboratories (St. Constant, QC, Canada). Rats were maintained under a constant photoperiod of 12L:12D and received food and water ad libitum. Rats were euthanized with CO_2 and cervical dislocation. Epididymides were frozen in liquid nitrogen, and tissues were stored at $-80°C$. All animals protocols used in this study were approved by the University Animal Care Committee.

Rapid Amplification of cDNA Ends

Total RNA was extracted from pooled proximal epididymides (initial segment, caput, and corpus) from two 25-day-old rats, using Illustra RNAspin mini-kit (GE Healthcare, Baie d'Urfe, QC, Canada), according to the manufacturer's instructions. The 5′ region of the *Gjb2* transcript was amplified using FirstChoice RNA ligase-mediated rapid amplification of cDNA ends (RLM-RACE) kit (Ambion, Austin, TX) according to the manufacturer's instructions. Gene-specific primer sequences used for these experiments are listed in Supplemental Table S1 (all Supplemental Data are available online at www.biolreprod.org). The first PCR amplification reaction consisted of using

the *Gjb2*-outer RACE primer and the 5′ RACE outer primer from the RNAspin mini-kit. Two nested PCRs were then conducted using the *Gjb2*-innerRACE1 primer and the *Gjb2*-innerRACE2 with the 5′RACE Inner primer from the kit. These primers were designed to amplify products of 221 and 171 bp, respectively. PCR amplifications were carried out at 94°C for 5 min, then 35 cycles at 94°C for 30 sec, 63°C for 30 sec, and 72°C for 30 sec. Products were analyzed using 2% agarose gels stained with ethidium bromide. Bands were excised, purified, and sent for sequencing (Genome Quebec, Montreal, QC, Canada).

Sequence Analysis

RACE products and promoter sequences were compared to rat genomic sequences by using Basic Local Alignment Search Tool (BLAST; GenBank; http://blast.ncbi.nlm.nih.gov/). Determination of putative transcription factor binding sites located on the *Gjb2* promoter was done using Transcription Element Search System database (University of Pennsylvania, Philadelphia, PA). EMBOSS Cpgplot software (European Bioinformatics Institute; http://www.ebi.ac.uk/Tools/seqstats/emboss_cpgplot/) was used to predict CpG islands, and primers for the PCR following bisulfite treatment were designed using MethPrimer software (http://www.urogene.org/methprimer).

Cloning

Total genomic DNA from adult Sprague-Dawley rat liver was extracted using GenElute mammalian genomic DNA purification kit (Sigma-Aldrich, Oakville, ON, Canada), according to the manufacturer's instructions. Primers used for PCR amplification of the *Gjb2* promoter are shown in Supplemental Table S1. A 1697-bp fragment (-1564 to $+133$ relative to the transcription start site of *Gjb2*) of the 5′ region of the *Gjb2* promoter was amplified by PCR (5 min at 94°C, then 35 cycles for 30 sec at 94°C, 30 sec at 61°C, and 2.5 min at 72°C). The PCR amplicon was visualized using a 0.7% agarose gel stained with ethidium bromide. The DNA band of interest was excised, purified using ZymoClean gel DNA recovery kit (Zymo Research, Irvine, CA), and sequenced using an automated sequencer (Genome QC). The *Gjb2* promoter was ligated into the *Nhe*I and *Hind*III cloning sites of the pGL3-basic vector using T4 DNA ligase (New England Biolabs, Whitby, ON, Canada) upstream of the firefly luciferase gene (construct $-1564/+133$). After transformation of chemically competent bacteria (TOP10; Invitrogen, Burlington, ON, Canada), the plasmid was amplified, isolated, and sequenced.

Deletion constructs were generated by restriction digests of the first construct ($-1564/+133$) using *Nhe*I located upstream of the promoter and one of the unique restriction sites (*Avr*II, *Spe*I, and *Pst*I) present along the promoter sequence. The resulting linearized DNA fragments deleted for different 5′ fragments of the promoter were then purified by agarose gel electrophoresis, filled in using T4 DNA polymerase (New England Biolabs), and ligated with T4 ligase. Constructs containing $-1083/+133$ bp, $-402/+133$ bp, and $-283/+133$ bp relative to the transcriptional start site were also produced in this manner.

To further characterize the $-283/+133$-bp region of the promoter, additional constructs were generated by PCR, using primers which contained specific restriction sites (Supplemental Table S1). PCR products were digested using *Hind*III and *Xho*I or *Nhe*I and separated by agarose gel electrophoresis, purified, and ligated into the pGL3-basic vector. Five constructs were generated: $-230/+133$, $-148/+133$, $-101/+133$, $-64/+133$, and $-8/+133$. Chemically competent bacteria were transformed with each of the constructs. Resulting clones were analyzed by restriction digest and sequenced (Genome QC). After constructs' identities were confirmed, they were purified using a commercial kit (Plasmid Midi kit; Qiagen, Toronto, ON, Canada) and stored at $-20°C$.

SP1 (-221; -126; -50 bp) and TFAP2A (-201; -124 bp) transcription factor binding sites were mutated from the $-283/+133$ construct by using QuickChange II site-directed mutagenesis kit (Stratagene, La Jolla, CA). A mutant construct was generated for the SP1/TFAP2A overlapping site (-126 to -116) and was used to produce a double mutant with the SP1 binding site located at -50 bp relative to the transcriptional start site. Polyacrylamide gel electrophoresis-purified mutagenic oligonucleotides (Integrated DNA Technologies, Toronto, ON, Canada) are detailed in Supplemental Table S1. Resulting clones were sequenced (Genome QC), and constructs were purified (plasmid midi-kit; Qiagen).

Cell Culture, Transfection, and Luciferase Assay

RCE-1 cells [40] were cultured in Dulbecco modified Eagle medium/Ham nutrient mixture F12 (Sigma-Aldrich) supplemented with 2 mM L-glutamine, 10 μg/ml insulin, 10 μg/ml transferrin, 80 ng/ml hydrocortisone, 10 ng/ml

epidermal growth factor, 10 ng/ml cAMP, and 5 nM testosterone at 32°C in a humidified chamber with 5% CO_2. Cells were cultured using mouse 24-well plates coated with collagen IV (BD Biosciences, Mississauga, ON, Canada). After 24 h, cells were washed with phosphate-buffered saline (PBS), and medium was replaced. Cells were transfected with both specific *Gjb2*-pGL3 constructs (1 µg) and a phRL-TK vector (100 ng; Promega, Madison WI), which was used as a control for transfection efficiency, using 3 µl of FastFect transfection reagent (Feldan, Quebec, QC, Canada) in 100 µl of medium. phRL-TK vector expresses *Renilla* luciferase under the control of the herpes simplex virus thymidine kinase promoter. A pGL3-basic empty vector was used as the negative control. A plasmid containing the luciferase gene under the control of the Rous sarcoma virus long terminal repeat (pRSV-Luc) was used as a positive control. Cells were placed in a CO_2 incubator for 24 h. The next day, medium was removed, and cells were washed with PBS. Cells were trypsinized, scraped, and transferred to clean 1.5-ml tubes. After centrifugation ($300 \times g$) for 10 min, cells were resuspended in 75 µl of medium and placed in an opaque 96-well plate (Corning Co, Corning, NY). Firefly and *Renilla* luciferase activities were determined using Dual-Glo luciferase assay system (Promega) and a MicroBeta Tri-Lux luminometer (PerkinElmer, Waltham, MA). All experiments were done in triplicate.

Electrophoretic Mobility Shift Assay

Nuclear extracts were prepared from RCE-1 cells and proximal epididymides (initial segment, caput, and corpus) of 25- and 42-day-old rats, using a commercial nuclear extract kit (Active Motif, Carlsbad, CA). Protein concentrations were determined using the BCA protein assay kit (Pierce; Thermo Fisher Scientific, Waltham, MA). Sequences of oligonucleotides containing the overlapping SP1/TFAP2A site and the proximal SP1 site used for electrophoretic mobility shift assay (EMSA) are shown in Supplemental Table S1. A 10 pmol aliquot of sense oligonucleotides were end-labeled with 50 µCi of [γ-32P]ATP by using T4 polynucleotide kinase (5 units) in buffer (New England Biolabs) and incubated for 45 min at 37°C. Labeled oligonucleotides and their antisense strands were heated at 65°C for 10 min. A 2.5 molar excess of antisense oligonucleotide was added to each of the labeled oligonucleotides and incubated for 30 min at room temperature. The double-stranded oligonucleotides were purified using a Sephadex G-50 column (Nick column; GE Healthcare), and a 2-µl aliquot of the resulting fraction was analyzed for radioactivity. The specific activity of each purified fraction was greater than 5000 cpm/fmol. A 5-µg aliquot of nuclear protein extract (three separate pools of three 25-day-old rats and of two 42-day-old-rats) was mixed with 1× binding buffer (10 mM Tris-HCl, pH 7.5, 4% glycerol, 1 mM MgCl2, 0.5 mM EDTA, 50 mM NaCl, 0.5 mM DTT) and poly(dI-dC) (50 µg/ml). For competition or supershift experiments, unlabeled oligonucleotides or antibodies (1–5 µg) were added and incubated at room temperature for 30 min. The goat polyclonal anti-SP1 (product sc-59X; Santa Cruz Biotechnology, Dallas, TX) and rabbit polyclonal anti-TFAP2A (product sc-184X; Santa Cruz Biotechnology) antibodies were used for supershift experiments. Labeled oligonucleotides (30 fmol) were then added to the mixture and incubated for an additional 30 min at room temperature. Products were then separated using 6% polyacrylamide gels. Gels were dried and exposed overnight on autoradiographic films (Classic blue films; Universal X-Ray, Pointe Claire, QC, Canada).

Chromatin Immunoprecipitation

Chromatin immunoprecipitation (ChIP) was performed using the EZ-ChIP kit (EMD Millipore, Billerica, MA). RCE-1 cells were grown to confluence in 58-cm^2 culture dishes coated with collagen IV (BD Biosciences). Cells were fixed with 1% formaldehyde for 8 min at room temperature and quenched with 125 mM glycine. The cell layer was washed twice with ice-cold PBS and then recovered by scraping in 4 ml of ice-cold PBS supplemented with a protease inhibitor cocktail (EMD Millipore). Following centrifugation ($700 \times g$ for 5 min at 4°C), cells (5×10^6 cells/ml) were resuspended and lysed in SDS lysis buffer (1% SDS; 10 mM EDTA, and 50 mM Tris, pH 8) for 10 min and stored at −80°C. Lysates were thawed on ice and sonicated with 35 pulses of 15 sec on/45 sec off by using a Q125 sonicator (Qsonica, Newtown, CT) equipped with a 2-mm microtip probe. The chromatin was sheared into 200- to 1000-bp fragments and verified by agarose gel electrophoresis.

One million cell equivalents (200 µl of lysate) were used for each immunoprecipitation. A fraction of the precleared sample (12 µl) was kept as the input sample (1.2%). Chromatin was precleared for 1 h at 4°C and then incubated overnight at 4°C with 5 µg of SP1 (sc-59X; lot G1813; Santa Cruz Biotechnologies) or TFAP2A (sc-184X; lot J1110; Santa Cruz Biotechnology) antibodies. Positive and negative controls included in the kit were also performed to assess the kit's performance. Antibody-protein-DNA complexes were then precipitated using G protein agarose beads. The beads were washed in buffer, eluted, and the DNA purified according to the manufacturer's instructions (EMD Millipore).

PCR amplifications were then performed using the *Gjb2* ChIP primer pair (Supplemental Table S1), which amplified a 138-bp promoter region of the *Gjb2* gene encompassing the SP1 and TFAP2A/SP1 response elements. A 5-µl aliquot of DNA was used in a 25-µl volume reaction consisting of 0.5 µM of each primer, 0.2 mM deoxyribonucleotide triphosphates (dNTPs) (Invitrogen), 2 mM MgCl2, Mango *Taq* buffer and 1 U of Mango *Taq* DNA polymerase (Bioline, Taunton, MA). DNA was then amplified by PCR (denaturation at 94°C for 5 min, then 35 cycles of 94°C for 30 sec, 63°C for 30 sec, and 72°C for 30 sec). PCR products were separated using a 2% agarose gel stained with ethidium bromide.

Quantitative ChIP

Proximal epididymides (initial segment, caput, and corpus) from 25- and 42-day-old rats were crushed in liquid nitrogen using a mortar and pestle and fixed with 1% formaldehyde for 8 min at room temperature with gentle rotation. The reaction was quenched with the addition of glycine (125 mM), and tissues were centrifuged at $1250 \times g$ for 10 min at 4°C. Pellets were washed twice with PBS and resuspended in cytoplasmic buffer (10 mM Tris pH 7.4; 3 mM $CaCl_2$; 3 mM MgCl2; 1 mM PMSF; and protease inhibitor cocktail; Sigma-Aldrich). Samples were then homogenized with a dounce homogenizer on ice, centrifuged ($850 \times g$) for 10 min at 4°C, and resuspended in cytoplasmic buffer. Samples were manually dounced with 0.6 % nonyl phenoxypoly-ethoxylethanol (NP40), using a glass homogenizer to yield a single-cell suspension. Nuclei were recovered by centrifugation at $14\,000 \times g$ for 1 min at 4°C. Pellets were resuspended in SDS lysis buffer (100 mg/ml) and stored at −80°C until sonication. Nuclei were sonicated on ice with 30 pulses of 30 sec on and 20 sec off. Chromatin analysis was performed as described above. Protein concentrations were determined using Pierce BCA protein assay kit (Thermo Fisher Scientific). Immunoprecipitation was done using 150 µg of protein as described above, using 5 µg of SP1, TFAP2A, or KLF4 (sc-20691; lot H0514; Santa Cruz Biotechnology) antibodies.

Quantification was done by qPCR, using *Gjb2* ChIP primers (Supplemental Table S1). These primers amplified a 238-bp region of the *Gjb2* gene promoter encompassing SP1, TFAP2A, and KLF4 response elements. These analyses were done using a 2 µl-aliquot of DNA in 15 µl of PerfeCTa SYBER Green Supermix (Quanta Biosciences, Gaithersburg, MD) and 0.3 µM of each primer. The DNA was then amplified by denaturation at 94°C for 5 min, followed by 40 cycles of 94°C for 30 sec, 63°C for 30 sec, and 72°C for 30 sec. Data were analyzed and normalized using the percent input method [41]. Data are percentages of positive control (input).

RNA Interference

Small interfering RNA (siRNA) against SP1 and TFAP2A (5 and 10 nM; Qiagen) and a scramble, or nonsense, siRNA (control; 5 and 10 nM; Qiagen) were transfected into RCE-1 cells using Lipofectamine RNAiMax (Thermo Fisher Scientific) according to the manufacturer's instructions. Cells were seeded onto 24-well plates and transfected 24 h later with siRNA. Cells were incubated for 24 h with siRNA against TFAP2A and for 48 h with siRNA against SP1. Cells were lysed, and total RNA was extracted using NucleoSpin RNA extraction kit (Macherey-Nagel, Bethlehem, PA) following the manufacturer's instructions. A 400-ng aliquot of total RNA was reverse transcribed using qScript cDNA super-Mix (Quanta Biosciences). Levels of *Sp1*, *Tfap2a*, and *Gjb2* were monitored by RT-qPCR as described above, using primers described in Supplemental Table S1. Levels of SP1, TFAP2A, and histone H3 protein were measured by Western blotting.

Western Blot Analyses

Nuclear proteins were extracted from 25- and 42-day-old rat epididymides, as described above. Protein concentrations were determined using Pierce BCA protein assay kit (Thermo Fisher Scientifc). Samples were stored at −80°C until electrophoresis. Proteins (25 µg) were diluted in Laemmli buffer and heated for 5 min at 94°C. Proteins were then separated by polyacrylamide gel electrophoresis on a 4%-to-20% gradient gels and transferred onto a polyvinylidene fluoride membrane by using a Transblot apparatus (Bio-Rad Laboratories, Mississauga, ON, Canada). Membranes were blocked for 1 h with 5% nonfat milk powder dissolved in Tris-buffered saline containing 0.1% Tween-20 (TBST) at room temperature. Membranes were then incubated overnight at 4°C with rabbit anti-TFAP2 (2 µg/ml) or goat anti-SP1 (2 µg/ml) or rabbit anti-histone 3 (2 µg/ml; catalog no. 4499; Cell Signaling, Danvers, MA) antibodies in blocking solution. After a series of washings in TBST, membranes were incubated for 1 h at room temperature with horseradish peroxidase-conjugated goat anti-rabbit IgG (0.04 µg/ml; product sc-2004; Santa

Cruz Biotechnology) or with donkey anti-goat IgG (0.04 μg/ml; product sc-2020; Santa Cruz Biotechnology). Signals were revealed using Clarity Western enhanced chemoluminescence substrate (Bio-Rad) and analyzed using a ChemiDoc MP imaging system (Bio-Rad).

Bisulfite Treatment

Total genomic DNA (gDNA) from the proximal epididymides of 25- and 42-day-old rats was extracted using GenElute mammalian genomic dna purification kit (Sigma-Aldrich). The bisulfite treatment was performed using EZ DNA methylation kit (Zymo Research). The conversion reagent was added to 500 ng of gDNA and incubated for 16 h at 50°C in the dark. The resulting DNA was purified and amplified by PCR, using JumpStart *Taq* DNA polymerase (Sigma-Aldrich) and bisulfite primers (Supplemental Table S1). Primers were designed to amplify two regions of the *Gjb2* promoter: region 1, which consists of nucleotides from −194 to +97, whereas region 2 was located from −700 to −483 bp relative to the transcriptional start site.

The methylation of the *Rhox5* promoter [42] was used as a positive control for the bisulfite treatment. The program used to amplify the region from −402 to −111 bp was 94°C for 1 min, 35 cycles at 94°C for 30 sec, 59°C for 30 sec and 72°C for 1 min with a final extension step at 72°C for 7 min. PCR products were analyzed on a 2% agarose gel and products were excised and purified. Products were cloned using the pGME-T Easy Vector system (Promega). Clones generated from epididymides of rats at each of two ages were sequenced (Genome Quebec) and their methylation status determined.

Statistical Analysis

All statistical tests were performed using Prism software (GraphPad, San Diego, CA). One-way ANOVA followed by the Newman-Keuls post hoc test or Student *t* test were used to analyze data. A *P* value of <0.05 was considered significant.

RESULTS

Identification of One Transcription Start Site for the Gjb2 Gene in the Epididymis

To identify the transcriptional start site of the *Gjb2* gene, 5′ RLM-RACE was done using RNA from epididymides of 25-day-old rats. Sequential PCR of the cDNAs using the outer primers and subsequently the nested primers generated the predicted 221 and 171 bp products (Fig. 1). Sequencing and
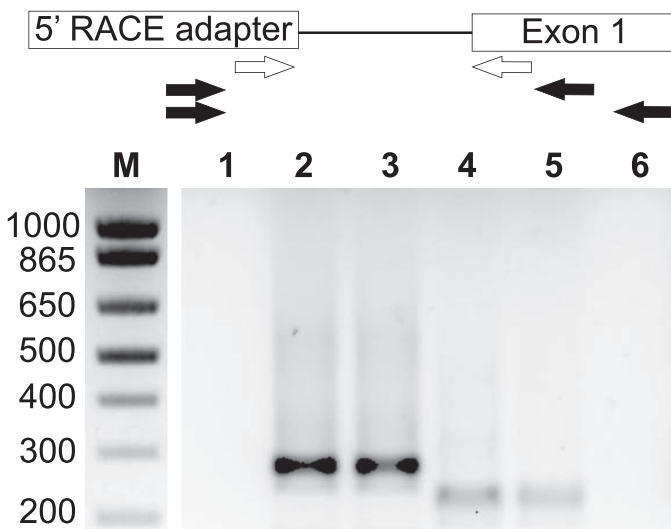

FIG. 1. 5′ RLM-RACE experiment revealed one transcriptional start site for the *Gjb2* gene. Amplification of the 5′-UTR ends was obtained by RLM-RACE. Schematic indicating the amplification strategy is shown. Nested PCR was performed using a first *Gjb2* specific-reverse primer on RNA from two pools of 25-day-old rats (lanes 2 and 3). A second nested PCR was performed (lanes 4 and 5). Control conditions were performed using water (lanes 1 and 6).

BLAST analysis using GenBank (National Center for Biotechnology Information, Bethesda, MD) confirmed the identity of the products. Results showed the presence of one single transcription start site for *Gjb2* gene in the epididymis, which was determined to be an adenine at position −3829 bp relative to the ATG start codon (Fig. 2A).

The *Gjb2* proximal promoter is located within a CpG island that begins at −201 and extends to +237 bp relative to the transcriptional start site (Fig 2B). Sequence analysis of the *Gjb2* promoter revealed several predicted transcription factor binding sites. Three SP1, 2 TFAP2A, and 4 KLF4 binding sites were identified in the 230-bp upstream sequence relative to the previously characterized transcriptional start site (Fig. 2A). SP1 and TFAP2A transcription factors are typical of CpG islands as they bind GC-rich regions. An overlapping site of the two transcription factors was also at position −126 to −136 bp relative to the transcriptional start site. This site has been previously identified as being important for the transcriptional activity of *Gjb2* in the rat mammary gland [31].

Gjb2 Promoter Activity

Using specific primers (Supplemental Table S1) and a luciferase promoterless reporter vector (pGL3), a 1697-bp fragment of the *Gjb2* promoter was isolated and cloned. This fragment contained 1564 bp of upstream and 133 bp of downstream transcriptional start site as identified by RLM-RACE. In order to identify the core promoter of the *Gjb2* gene, 5′ deletion constructs were generated and transfected into RCE-1 cells (Fig 3A). The full-length construct (−1564/+133) and the first 5′ digested construct (−1083/+133) presented elevated luciferase activity with a 7- and 9-fold increase, respectively, compared to the promoterless vector pGL3. The highest promoter activity was obtained with the −402/+133 and −283/+133 constructs, which showed 15- and 14-fold increased luciferase activity compared to the empty pGL3 vector. Additional 5′ deletion of the promoter with the −101/+133 construct resulted in a dramatic decrease in luciferase activity, suggesting the presence of essential regulatory elements within the −283 to −101 bp region relative to the transcriptional start site.

In order to map and characterize regulating regions of the first 283 bp of the proximal *Gjb2* promoter, four additional constructs were generated by 5′ deletion of the −283/+133 construct (Fig. 3B). The first deletion, −230/+133, showed an increase of the transactivation activity compared to the −283/+133 construct. Transfection of the other three deletion constructs, −148, −64, and −8/+133, resulted in decreased luciferase activity, which was completely lost in the −8/+133 construct. Each of these deletion constructs is associated with the loss of a putative SP1 or TFAP2A binding site, suggesting a role for these transcription factors in the activation of the *Gjb2* promoter.

Role of SP1 and TFAP2A Putative Binding Sites in RCE-1 Cells

To confirm the roles of SP1 and TFAP2A in the transactivation of the *Gjb2* promoter, site-directed mutagenesis of the SP1 and TFAP2A putative binding sites was performed. Seven mutagenesis constructs were obtained and transfected into RCE-1 cells (Fig 4). Mutation of the SP1 and TFAP2A sites located at −221 and −201bp, respectively, showed no differences in luciferase activity compared to the nonmutated constructs. However, mutation of the SP1 sites located at −50 and −126 bp and the TFAP2A site located at −124 bp relative
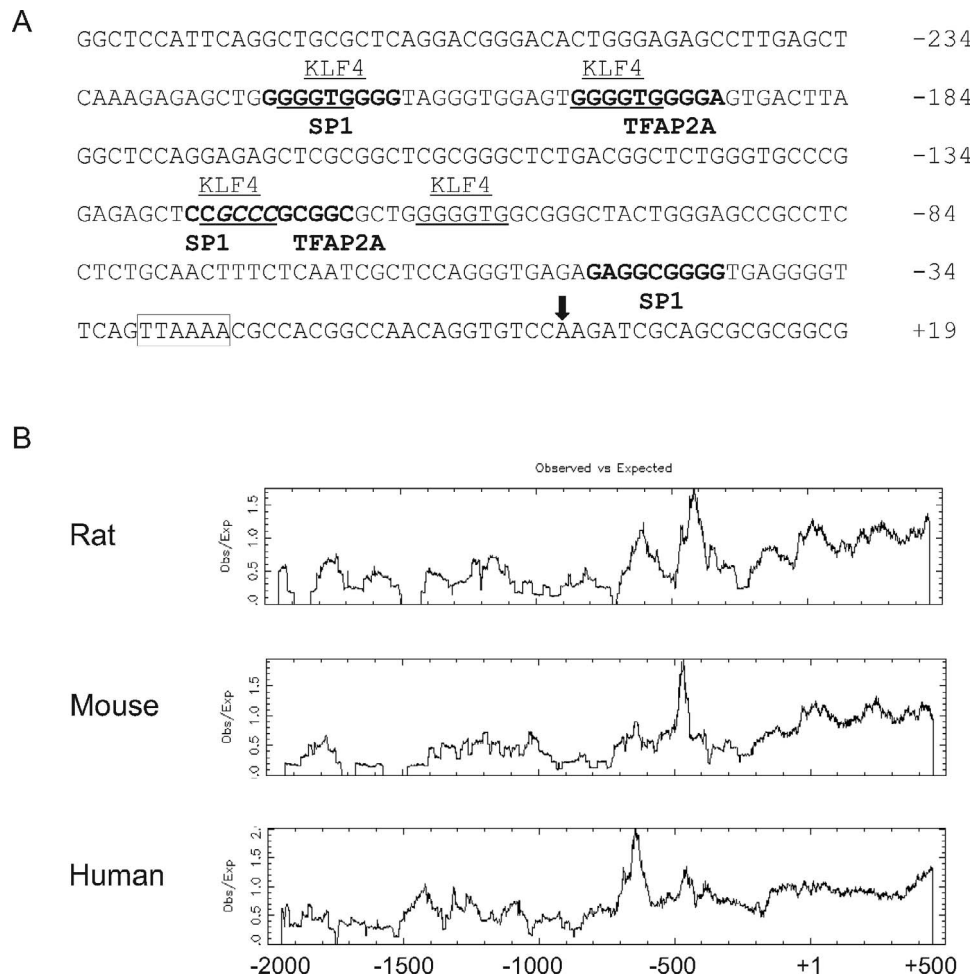
A

```
GGCTCCATTCAGGCTGCGCTCAGGACGGGACACTGGGAGAGCCTTGAGCT      -234
                KLF4                         KLF4
CAAAGAGAGCTGGGGGTGGGGTAGGGTGGAGTGGGGTGGGGAGTGACTTA      -184
              SP1                         TFAP2A
GGCTCCAGGAGAGCTCGCGGCTCGCGGGCTCTGACGGCTCTGGGTGCCCG      -134
              KLF4                  KLF4
GAGAGCTCCGCCCGCGGCGCTGGGGGTGGCGGGCTACTGGGAGCCGCCTC      -84
        SP1       TFAP2A
CTCTGCAACTTTCTCAATCGCTCCAGGGTGAGAGAGGCGGGGTGAGGGGT      -34
                                      SP1
TCAGTTAAAACGCCACGGCCAACAGGTGTCCAAGATCGCAGCGCGCGGCG     +19
```

B

FIG. 2. Schematic representation of the *Gjb2* promoter containing the proximal CpG island. **A**) The transcriptional start site (tss) was identified by RLM-RACE (arrow). Sequence analysis of the *Gjb2* promoter using TRANS-FAC and TFSearch software revealed multiple putative SP1 and TFAP2A binding sites (bold characters). An overlap of a TFAP2A and SP1 binding site is shown (italic characters). Putative KLF4 binding sites are shown (underlined). The rectangle indicates the TATA box-like sequence. **B**) A conserved CpG island is located in the first 500 bp upstream of the tss and continues into exon 1, which is downstream from the transcriptional initiation site in rat, mouse, and human *Gjb2* gene promoter region. CpG plot software was used to locate the CpG island in the *Gjb2* promoter from different species. +1 = transcriptional start site.

to the transcriptional start site significantly decreased transactivation of the reporter gene. Furthermore, mutation of the overlapping SP1/TFAP2A binding site also resulted in decreased luciferase activity. Double mutation of response elements for the overlapping SP1/TFAP2A and SP1 binding site at position −50 bp completely abolished the luciferase activity, suggesting a crucial role of these binding sites for the transactivation of *Gjb2* gene in the epididymis.

Binding of SP1 and TFAP2A to the Gjb2 Promoter

Recruitment of SP1 and TFAP2A transcription factors to the *Gjb2* promoter in vivo was confirmed by ChIP assays using chromatin from RCE-1 cells and from epididymides of 25- and 42-day-old rats. Immunoprecipitation with anti-SP1 or anti-TFAP2A antibody confirmed that both transcription factors bound to the *Gjb2* promoter in RCE-1 cells (Fig 5A).

To confirm the levels of these transcription factors recruited to the promoter in tissue, quantitative ChIP assays were performed using epididymal nuclear protein from 25-day-old and 42-day-old rats. Results showed that both SP1 and TFAP2A were recruited to the *Gjb2* promoter in epididymides from 25-day-old rats (Fig 5B). Interestingly, recruitment of TFAP2A to the *Gjb2* promoter was significantly decreased in

42-day-old rats. Although SP1 recruitment was also decreased on the *Gjb2* promoter of the older rats, this decrease was not statistically significant ($P = 0.1143$). These results are consistent with the decreased expression of *Gjb2* mRNA previously observed in older rats.

In order to determine if SP1 and TFAP2A bound to the putative sites previously identified on the *Gjb2* promoter, EMSA assays using nuclear proteins were performed. Nuclear proteins bound specifically to double-stranded oligonucleotides corresponding to the proximal SP1 response element (−50 bp) on the *Gjb2* promoter (Fig. 6A; Supplemental Table S1). High molecular weight complexes, particularly intense in RCE-1 cell extracts, were out-competed by an excess of cold competitor but not by an excess of cold competitor in which the SP1 site was mutated. Preincubation of nuclear extracts with an anti-SP1 antibody resulted in a decrease in protein-DNA complexes with nuclear proteins from both RCE-1 cells and tissue (Fig. 6B). A second double-stranded oligonucleotide containing the SP1/TFAP2A overlapping site (Supplemental Table S1) was used to detect protein-DNA complexes in both RCE-1 cells and tissue (Fig. 7). Again, complexes were particularly intense in RCE-1 cell nuclear extracts. Preincubation with anti-SP1 antibody resulted in a supershift in proteins from RCE-1 cell extracts and the prevention of the protein-DNA complexes formation in
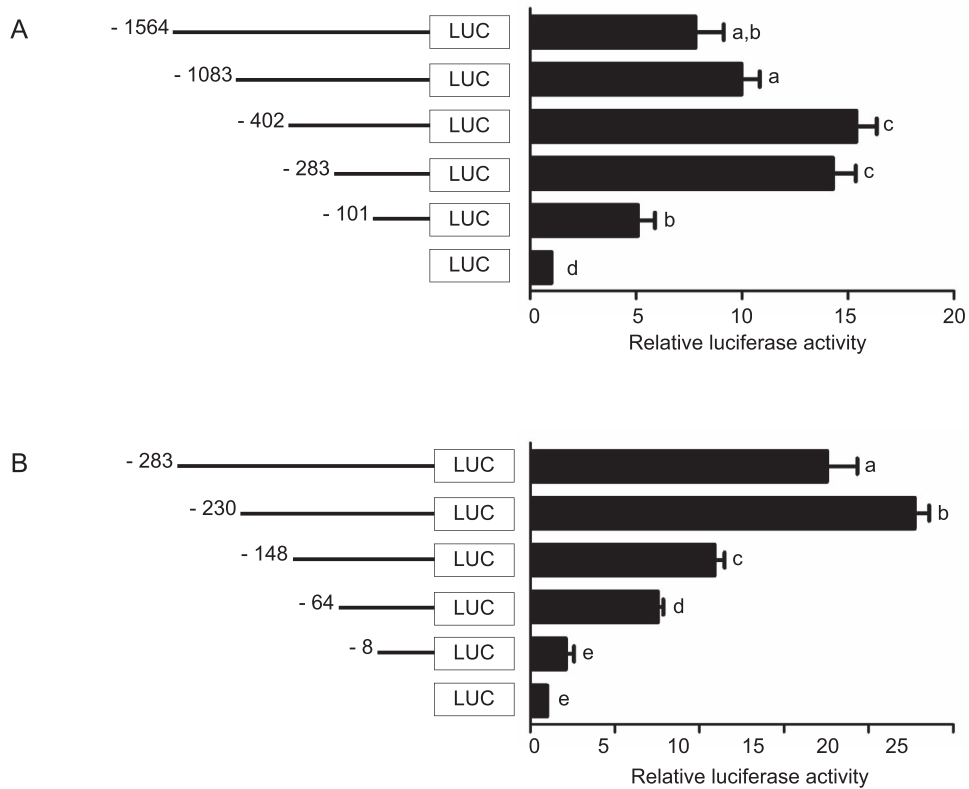
5

FIG. 3. *Gjb2* promoter activity in RCE-1 cells. **A**) Rat *Gjb2* promoter was amplified by PCR (−1564 bp relative to the transcription start site identified in RLM-RACE experiment) and cloned into the pGL3 basic luciferase reporter vector. Several promoter deletion constructs were obtained by restriction digests: −1083, −402, −283, and −101 bp. **B**) The −283 bp construct was further analyzed by successive deletions to produce four other constructs: −230, −148, −64, and −8 bp. RCE-1 cells were transfected with each construct and with the pHRL-TK vector to normalize for transfection efficiency. The promoterless pGL3 basic vector was used as a negative control. Data represent relative luciferase activity for the different constructs normalized to that of *Renilla* activity. Data are mean ± SEM; each analysis was done in triplicate. Statistical analysis was done using one-way ANOVA, followed by a Newman-Keuls comparison test. Different letters indicate significant differences ($P < 0.05$).
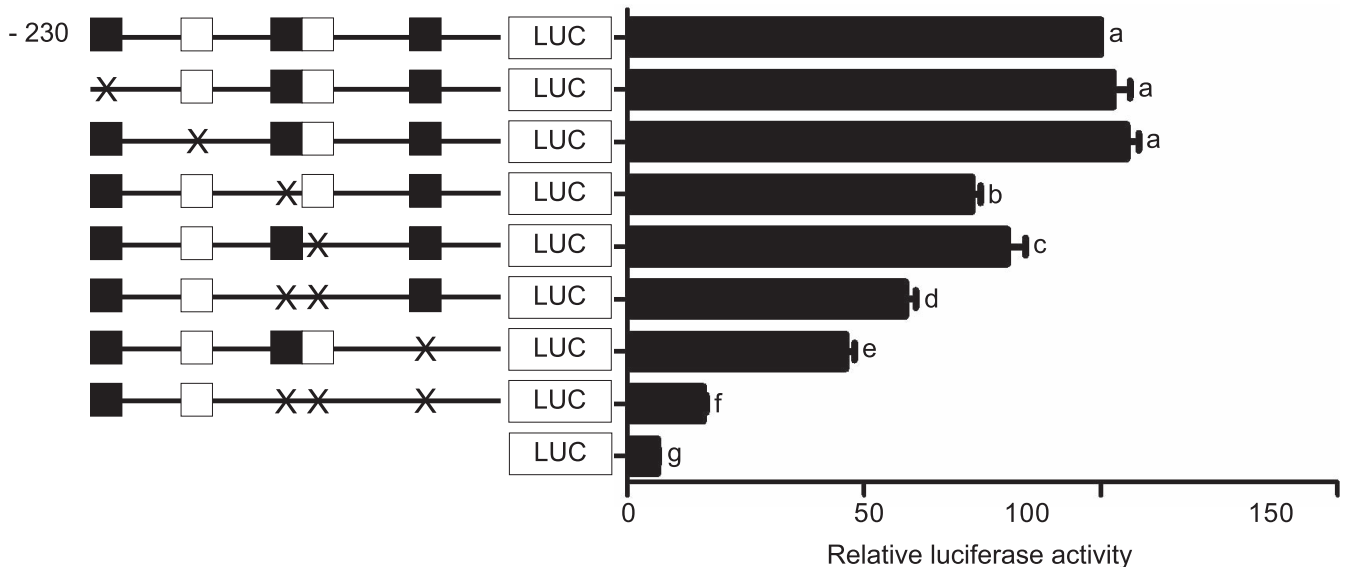

FIG. 4. SP1 and TFAP2A transcription factors are important for transcriptional activity of the *Gjb2* promoter. Putative binding sites SP1 and TFAP2A are represented in black and white boxes, respectively. Site-directed mutagenesis was performed using the −283 *Gjb2* reporter vector. RCE-1 cells were transfected with each of the seven point mutation constructs and with the pHRL-TK vector to normalize for transfection efficiency. The pGL3-basic empty vector was used as negative control. Firefly and *Renilla* luciferase activities were measured. Data are firefly-to-*Renilla* activity ratios. Data are mean ± SEM; each analysis was done in triplicate; n = 3 separate experiments. Statistical analysis was done using ANOVA, followed by a Newman-Keuls test. Different letters indicate significant differences ($P < 0.05$).
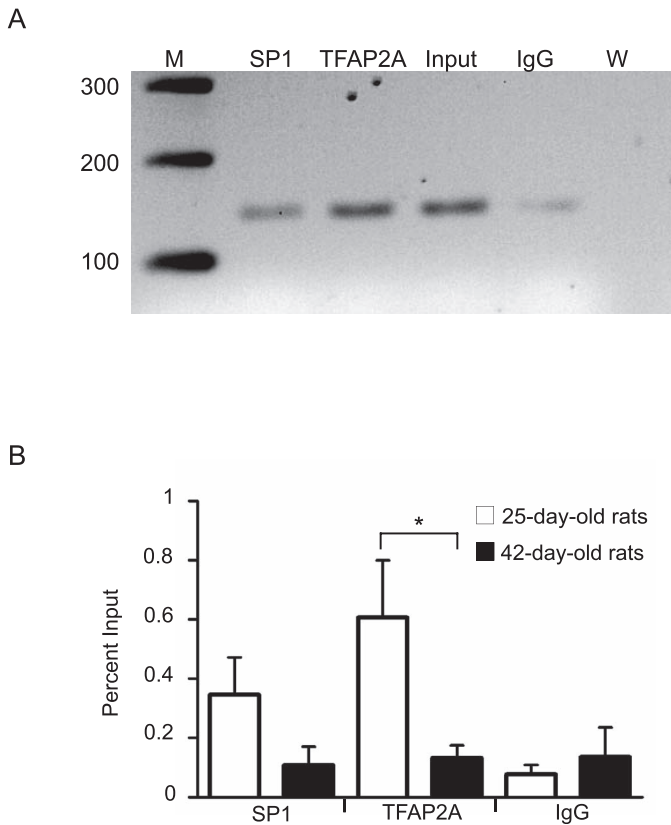
A

B

FIG. 5. SP1 and TFAP2A transcription factors interact with the *Gjb2* promoter. **A**) ChIP experiments were performed using RCE-1 cells. Chromatin was immunoprecipitated with either anti-SP1 and anti-TFAP2A antibodies or IgG (negative control). PCR reactions amplified a 138-bp fragment of the *Gjb2* promoter, and immunoprecipitation with SP1 or TFAP2A antibodies showed an enrichment compared to IgG. Data represent three separate experiments. W = water control; M = molecular weight ladder. **B**) Quantitative ChIP analyses were performed using chromatin from the epididymides of 25- and 42-day-old rats. qPCR showed a significant enrichment for immunoprecipitations with anti-SP1 and anti-TFAP2A antibodies for the *Gjb2* promoter region, compared to those of the IgG negative control in 25-day-old rats. Data are percentages of input. Data are mean ± SEM; n = 4 separate experiments. Statistical analysis was done using Student *t* test. *Significant differences ($P < 0.05$).

tissue (Fig. 8A). Preincubation with an anti-TFAP2A resulted in a decreased intensity of DNA-protein complexes in RCE-1 cells. A clear supershift band was apparent in epididymal tissues from younger and older rats, but only in overexposed films (Fig. 8B).

Role of SP1 and TFAP2A in the Transcriptional Activity of Gjb2 *in RCE-1 Cells*

To confirm the role of SP1 and TFAP2A in the regulation of *Gjb2* expression, siRNA were used to knock down these genes. Our data indicate that *Sp1* and *Tfap2a* mRNA levels were decreased by approximately 50% compared to those of control siRNA (Fig 9A). Western blot analyses showed that protein levels of TFAP2A and SP1 were 50% ($P < 0.005$) and 70% ($P < 0.0005$) decreased, respectively, compared to scramble siRNA (Fig 9B). RT-qPCR experiments showed that *Gjb2* mRNA levels were decreased by almost 60% when SP1 was knocked down ($P < 0.05$) (Fig. 9C). Interestingly, TFAP2A knockdown had no effect *Gjb2* mRNA levels (Fig. 9C).
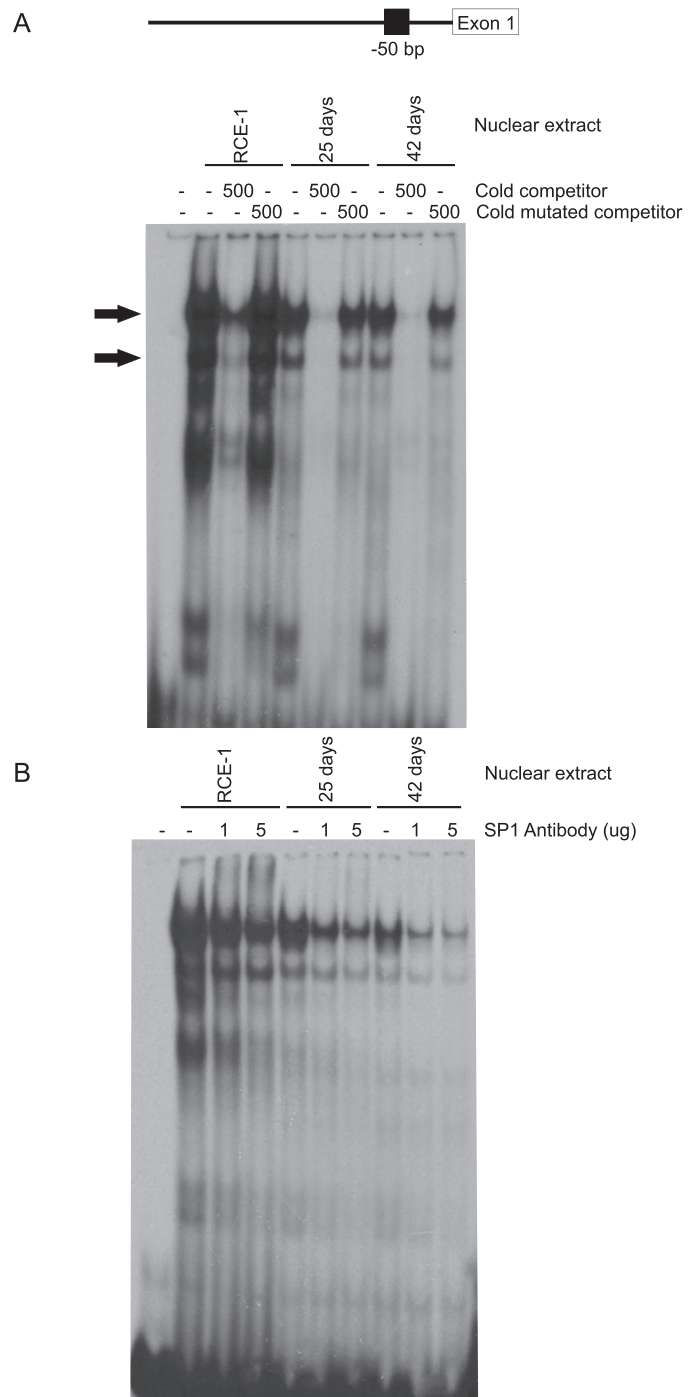
A

B

FIG. 6. SP1 binding to the proximal SP1 putative binding site (−50 bp) of the *Gjb2* promoter. EMSA was performed using the *Gjb2* promoter region containing the proximal SP1 binding site. Schematic of the SP1 binding site relative to exon 1 of the *Gjb2* promoter is shown. Nuclear extracts from RCE-1 cells, proximal epididymides of 25- and 42-day-old rats were incubated with radiolabeled double-stranded oligonucleotides containing the SP1 binding site. **A**) For competition studies, nuclear proteins were preincubated with 500 M excess of cold competitor or with cold oligonucleotides containing a mutated SP1 binding site. **B**) Supershift studies were performed by preincubating nuclear proteins with 1 or 5 μg of anti-SP1 antibody. Protein-DNA complexes are indicated by arrows.

SP1 and TFAP2A Protein Levels

To determine whether the decrease in SP1 and TFAP2A recruitment to the *Gjb2* promoter was due to a decrease in
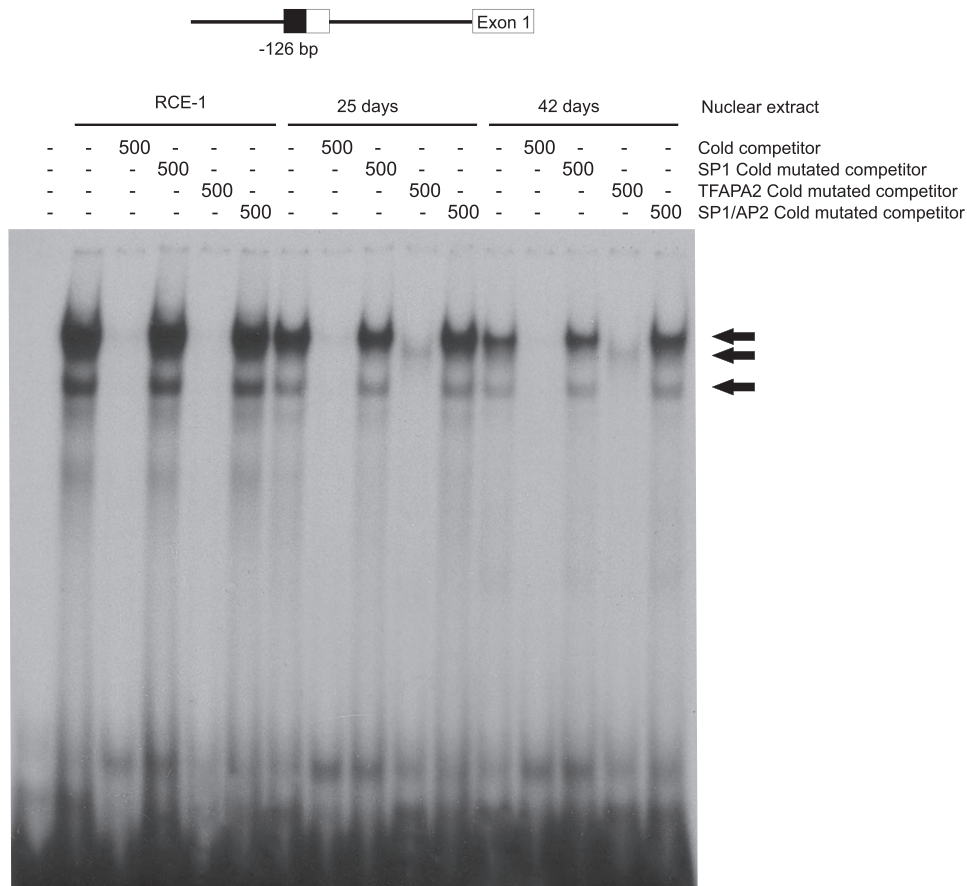
FIG. 7. SP1 and TFAP2A are shown binding to the putative SP1/TFAP2A overlapping binding site of the *Gjb2* promoter. EMSA was performed using the *Gjb2* promoter region containing the overlapping SP1/TFAP2A binding site. Schematic shows putative SP1/TFAP2A binding site relative to exon 1 of the *Gjb2* promoter. Nuclear extracts from RCE-1 cells, proximal epididymides of 25- and 42-day-old rats were incubated with radiolabeled double-stranded oligonucleotides containing the overlapping site. For competition studies, nuclear proteins were preincubated with 500 M excess of cold competitor or with cold oligonucleotides containing a mutation in the SP1 binding site or in the TFAP2 binding site or in both. Protein-DNA complexes are indicated by arrows.

levels of these factors in the epididymis, Western blots were analyzed using epididymal nuclear proteins from both 25- and 42-day-old rats. Western blot analyses revealed that the nuclear SP1 and TFAP2A protein levels were similar at 25 and 42 days of age (Fig. 10).

Methylation Status of the Gjb2 *Promoter*

The proximal region of the *Gjb2* promoter contains a CpG island (Fig. 2B). Studies have reported that methylation status can alter SP1 and TFAP2A binding [43, 44]. Therefore, the methylation status of the *Gjb2* promoter was examined. PCR was performed using bisulfite-transformed DNA on two regions of the *Gjb2* promoter region 1, consisting of nucleotides from -194 to $+97$, and region 2, from -700 to -483, relative to the transcriptional start site. There was no methylation of the 29 CpG sites present in region 1 of the *Gjb2* promoter (Fig 11B). For region 2, a slight increase in methylation status was observed between younger and older animals (Fig 11C). The percentage of methylated CpG sites was 25.47% in young animals, whereas it was 33.67% in older rats, representing an increase of 8.2% with age. The *Rhox5* promoter was chosen as a positive control for the bisulfite treatment because previous studies reported region-specific modifications of DNA methylation of this promoter during mouse epididymal development [42]. Our results in rat are

consistent with those observed during the differentiation of mouse proximal epididymis (Fig 11A) [42].

Role of KLF4 in the Regulation of Gjb2 *Expression*

KLF4 is a known repressor of GJB2 expression during keratinocyte differentiation [16, 45]. Our data indicate that KLF4 levels increase during epididymal development when *Gjb2* levels decrease (Fig. 12A). In order to assess the role of KLF4 on *Gjb2* expression during epididymal differentiation, recruitment of the transcription factor KLF4 on the *Gjb2* promoter was assessed by ChIP assay using chromatin of epididymides of 25- and 42-day-old rats. Chromatin was immunoprecipitated with an anti-KLF4 antibody, and no enrichment was observed for either age compared to IgG negative control (Fig 12B).

DISCUSSION

GJB2 is involved in crucial physiological processes by allowing the transfer of ions and small molecules, and deletion of this connexin in mice is lethal [46]. The expression of GJB2 differs among tissues and developmental stages, confirming its role in the differentiation process [26–28]. Dysregulation or mutation of the *Gjb2* gene leads to several pathologies [47],
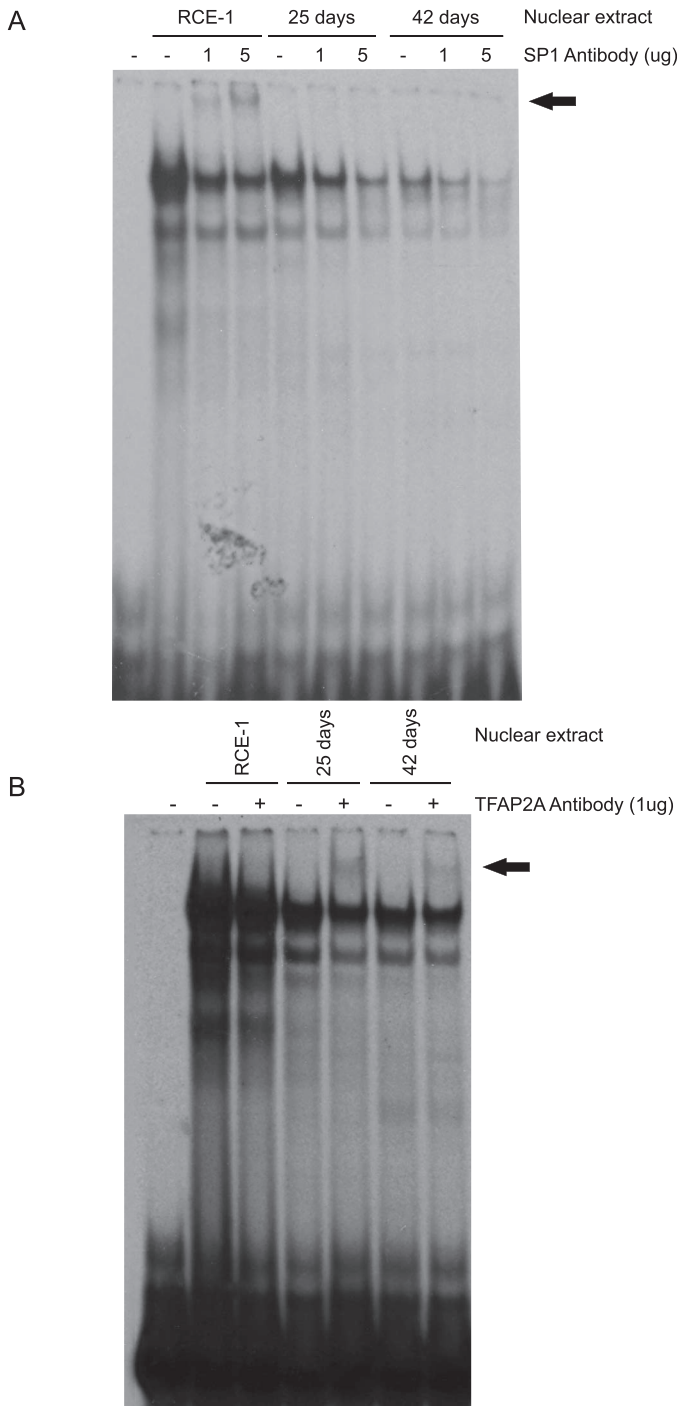
FIG. 8. Supershift of SP1 and TFAP2A binding to the putative overlapping binding site SP1/TFAP2A of the *Gjb2* promoter. Supershift studies were performed using the promoter region of *Gjb2* containing the overlapping binding site. **A**) Proteins were preincubated with (1 or 5 μg) anti-SP1 antibody. In RCE-1 cells, a supershift and decreased DNA-protein complexes are visible when nuclear proteins were preincubated with anti-SP1 antibody. In epididymal tissue, we observed a decrease in formation of DNA-protein complexes. **B**) Preincubation of nuclear proteins with anti-TFAP2A antibody (1 μg) resulted in a decrease in DNA-protein complexes in cells and in tissues. A distinct band was also observed in tissues treated with the antibody (arrow).

including cancer [36–38, 48, 49] and deafness [47, 50, 51] and skin pathologies [16, 52, 53].

The role of GJB2 in the epididymis is still poorly understood. We previously reported that GJB2 is present in the epididymis between adjacent cells that line the lumen of 21-day-old rats and between principal cells in 91-day-old rats [24]. GJB2 expression is dynamically regulated during postnatal development of rat epididymis. GJB2 is highly expressed during the early steps of differentiation but is barely detectable in adult epididymis [24]. Therefore, elucidation of the mechanisms regulating GJB2 expression provides an understanding of the mechanisms acting during the postnatal differentiation of the epididymis.

Results of this study demonstrate that the *Gjb2* gene in the rat epididymis has only one transcriptional start site, which we identified as an adenine, located 24 bp downstream of a TATA-like box. The TATA-like motif has been previously identified and is highly conserved in the rat, human, and mouse *Gjb2* promoters [29, 30, 32]. The *Gjb2* promoter is also located within a CpG island, which starts at −201 bp from the identified transcription start site and extends to +237 bp downstream. Mammalian promoters can be divided into two classes: TATA-box–enriched promoters and CpG-rich promoters [54]. Promoters that contain TATA boxes usually have one transcription start site, whereas CpG-rich promoters are more flexible and usually contain several transcriptional start sites [54]. The *Gjb2* promoter possesses a TATA-like motif and is located in a CpG island. Previous studies predicted 4 transcription start sites for the *Gjb2* gene in the rat mammary gland [30] and 2 in the mouse [55]: a strong transcriptional start site was identified as an adenine and a second weaker one located 7 bp downstream. Only one transcriptional start site has been identified in human for *Gjb2*, and as in the rat, it is an adenine [32]. Our results, combined with previous studies, show that the *Gjb2* promoter belongs to the two classes of promoters and confirms that there are differences in the transcriptional mechanisms which drive the expression of *Gjb2* between different tissues and species.

Luciferase assays indicated that our 1.5-kb construct of the *Gjb2* promoter contained sufficient information to drive expression of the reporter gene. A first series of deletions of the full-length construct revealed that the proximal 283-bp region of the *Gjb2* promoter was sufficient for transactivation of the reporter gene. In order to further characterize regulatory regions of the proximal 283-bp construct, another series of deletions was performed. The −230/+133 construct yielded a higher transactivation activity than the −283/+133 construct, suggesting the presence of a repressor site located within −283 and −230 bp region. Further deletions (−148, −64 and −8/+133) resulted in a significant decrease of the luciferase activity, suggesting the presence of essential regulatory elements within the proximal 230 bp.

The *Gjb2* promoter sequence showed multiple GC boxes that are specific for CpG islands. Several transcription factors, such as SP1 and TFAP2A, can bind to elements within GC boxes [56, 57]. Three SP1 putative binding sites were identified within these GC boxes at positions −221, −126, and −50 bp relative to the transcriptional start site. Two TFAP2A response elements were also located at positions −201 and −124 bp of the *Gjb2* promoter. A TFAP2A/SP1 overlapping site was located at positions −126 to −116 bp relative to the transcriptional start site. This overlapping site as well as the GC boxes of the proximal promoter of *Gjb2* have been previously reported and are evolutionarily conserved, suggesting that these are critical for the regulation of the *Gjb2* gene [31, 32]. Interestingly, we observed a decrease in the transactivation of the reporter gene with the deleted constructs −148, −64, and −8/+133, in which there is a loss of these putative binding sites. This emphasizes the importance of these transcription factors in the basal transcriptional activity of the
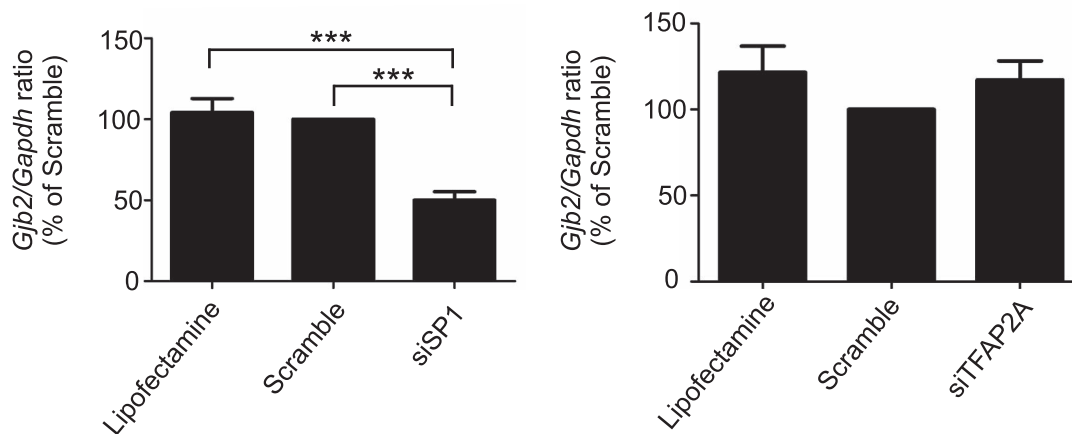
A
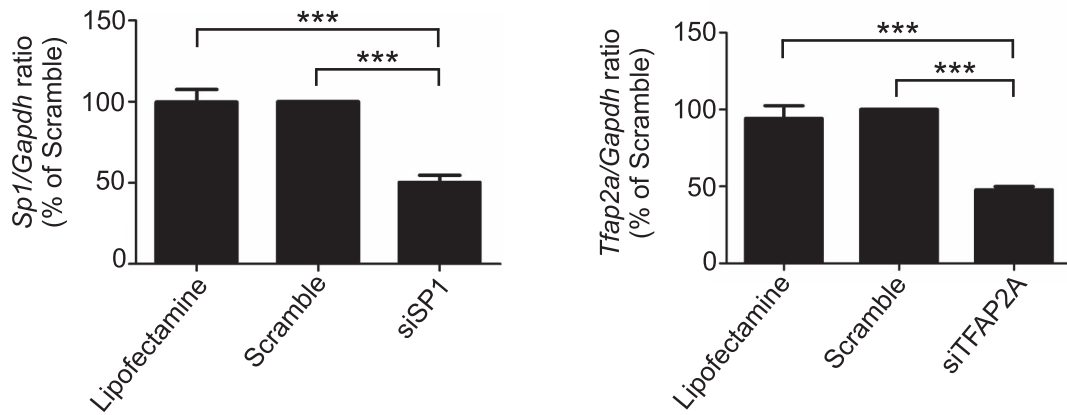
B
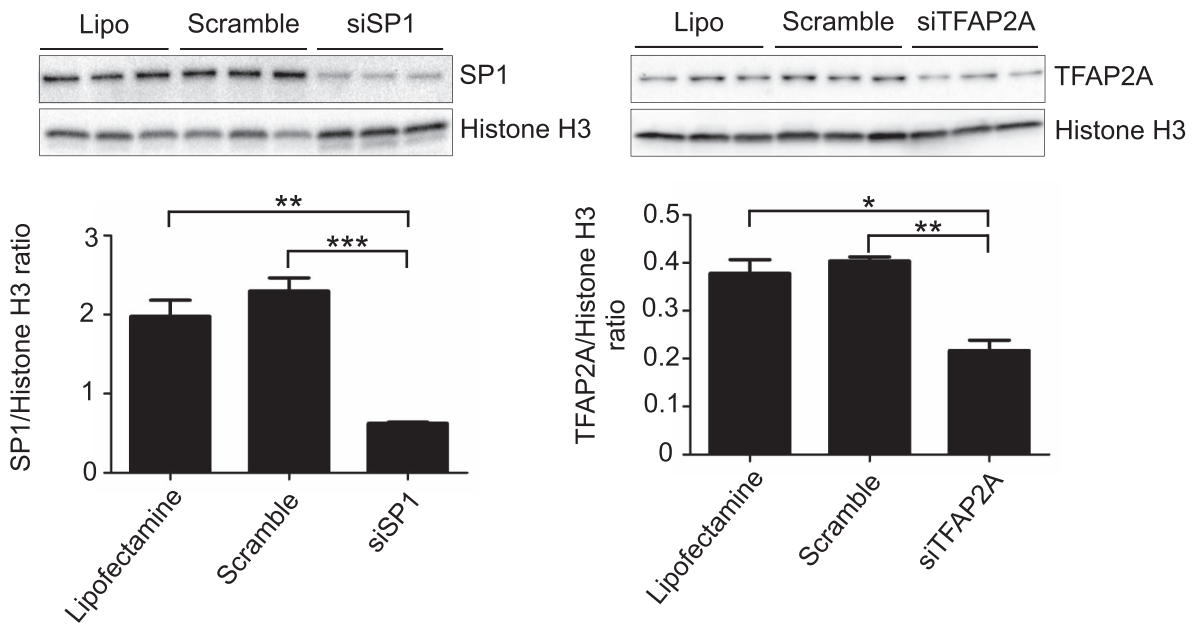
C

FIG. 9. SP1 and TFAP2A knockdown in RCE-1 cells. RCE-1 cells were transfected with either scramble (5 or 10 nM; 24 or 48 h), anti-SP1 (siSP1; 10 nM; 48 h), or anti-TFAP2A (siTFAP2A; 5nM; 24 h) siRNA. **A**) Total RNA was extracted, and RT-qPCR was used to measure mRNA levels of *Sp1* and *Tfap2a*, normalized to *Gapdh*. A significant decrease in mRNA for both transcripts was observed following treatment with specific siRNA. **B**) Levels of SP1 and TFAP2A proteins were 70% and 50% decreased, respectively, in cells treated with specific siRNA relative to scramble siRNA. **C**) SP1 knockdown resulted in a significant decrease in *Gjb2* mRNA levels. TFAP2A knockdown had no effect on *Gjb2* mRNA levels. ***$P < 0.0005$; **$P < 0.005$; *$P < 0.05$.
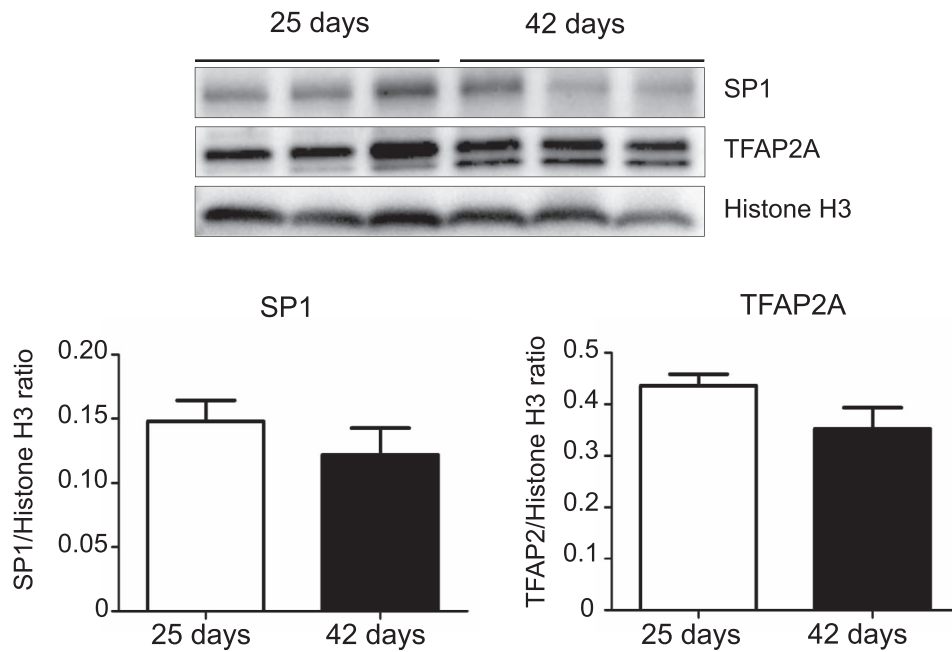
FIG. 10. SP1 and TFAP2A protein levels during development. Western blot analysis of nuclear SP1 and TFAP2A proteins in the proximal epididymis of 25- and 42-day-old rats is shown (n = 3). SP1 and TFAP2A nuclear protein levels were not different at either of the two ages. Nuclear protein levels were normalized to those of histone H3. Data are mean ± SEM.

Gjb2 gene in the epididymis. Directed mutagenesis experiments, EMSA, and ChIP assays confirmed the binding of SP1 on the *Gjb2* promoter in RCE-1 cells and in rat epididymis. These data indicate that both the TFAP2/SP1 overlapping site and the SP1 site located −50 bp upstream the transcriptional start site are crucial for the basal transcription of *Gjb2*, as the mutation of both of the sites almost completely abolishes the activity of the reporter gene. Because these sites are highly conserved among species, the binding and interaction of these transcription factors must be required for the transcriptional regulation of *Gjb2* [30, 31].

SP1 is a zinc-finger transcription factor ubiquitously expressed and whose response elements are often found within GC and GT boxes in a variety of gene promoters [58]. SP1 typically acts as an activator in mammalian cells [59]. Previous studies have identified SP1 as a regulator of *Gjb2* transcriptional activity. Tu et al. [29] showed that SP1 sites located at bp positions −81 and −93 were important for regulation of the human *Gjb2* gene in mammary cell lines. In rat mammary and uterine tissues, SP1 plays a critical role in the up-regulation of the *Gjb2* gene during pregnancy and lactation [30, 31]. In the epididymis, SP1 as well as SP3 are crucial for the expression of claudin 1, a tight junction protein implicated in the blood-epididymis barrier [60]. SP1 also binds to the promoter of the 5-α-reductase type 2 promoter, the enzyme responsible for the conversion of testosterone in dihydrotestosterone in the epididymis [61]. Thus, SP1 appears to play a role in the regulation of several genes involved in epididymal function.

TFAP2A is implicated in the regulation of various developmentally regulated genes, and its deletion in mouse yields a lethal phenotype [62, 63]. In mammary epithelial cells, TFAP2A, along with SP1, is involved in the up-regulation of *Gjb2* during pregnancy and lactation, when the epithelium undergoes differentiation [31]. In the epididymis, TFAP2A is a co-factor of androgen receptor (AR) signaling, indicating a role for TFAP2A in the tissue-specific AR recruitment [64, 65].

ChIP showed that SP1 and TFAP2A are recruited to the promoter of the *Gjb2* gene in RCE cells and in the epididymis

of 25-day-old-rats. EMSA experiments confirmed the binding of SP1 and TFAP2A on the predicted putative binding sites.

Using siRNAs, we confirmed the importance of SP1 in the transcription of *Gjb2*. However, TFAP2A knockdown had no effect on *Gjb2* mRNA levels. These data suggest that, although the TFAP2A site of the SP1/TFAP2A appears to be important for driving the *Gjb2* gene, other proteins could also bind to this site. The TFAP2 family of transcription factors is composed of five members in which the DNA-binding domain is highly conserved [66]. Because these recognize the same putative DNA binding sequence [67], it is possible that another member of the TFAP2 family may bind to the SP1/TFAP2A overlapping site in RCE cells. Another possibility is that the mutation of the TFAP2A site hinders the SP1 binding site. Furthermore, as our ChIP experiments showed a recruitment of TFAP2A on the *Gjb2* promoter, it is possible that only a small amount of TFAP2A is required to enhance the transcription of *Gjb2* and that the 50% decrease in the TFAP2A protein levels obtained by siRNA treatment may not be sufficient to inhibit its regulation of the *Gjb2* promoter.

Quantitative ChIP analyses showed that both SP1 and TFAP2A recruitment is decreased as a function of age, although the SP1 decrease was not significant. This observation is correlated with the expression levels of GJB2 in the epididymis. *Gjb2* mRNA is highly expressed in the epididymis of young rats, when the epithelium is not fully differentiated, but is not detectable in adult rats with differentiated epithelium [24]. These results suggest that as GJB2 expression is decreased, there is a decrease in SP1 and TFAP2A recruitment to the *Gjb2* promoter. Interestingly, levels of nuclear SP1 and TFAP2A were not significantly different between young and older animals. This suggests that there are differences in either the DNA binding sites or in cofactors that may regulate the binding of the transcription factor to the promoter region of the *Gjb2* gene.

DNA methylation of the proximal CpG island was examined. Studies have reported an increase in DNA methylation of the *Gjb2* gene promoter and *Gjb2* silencing in
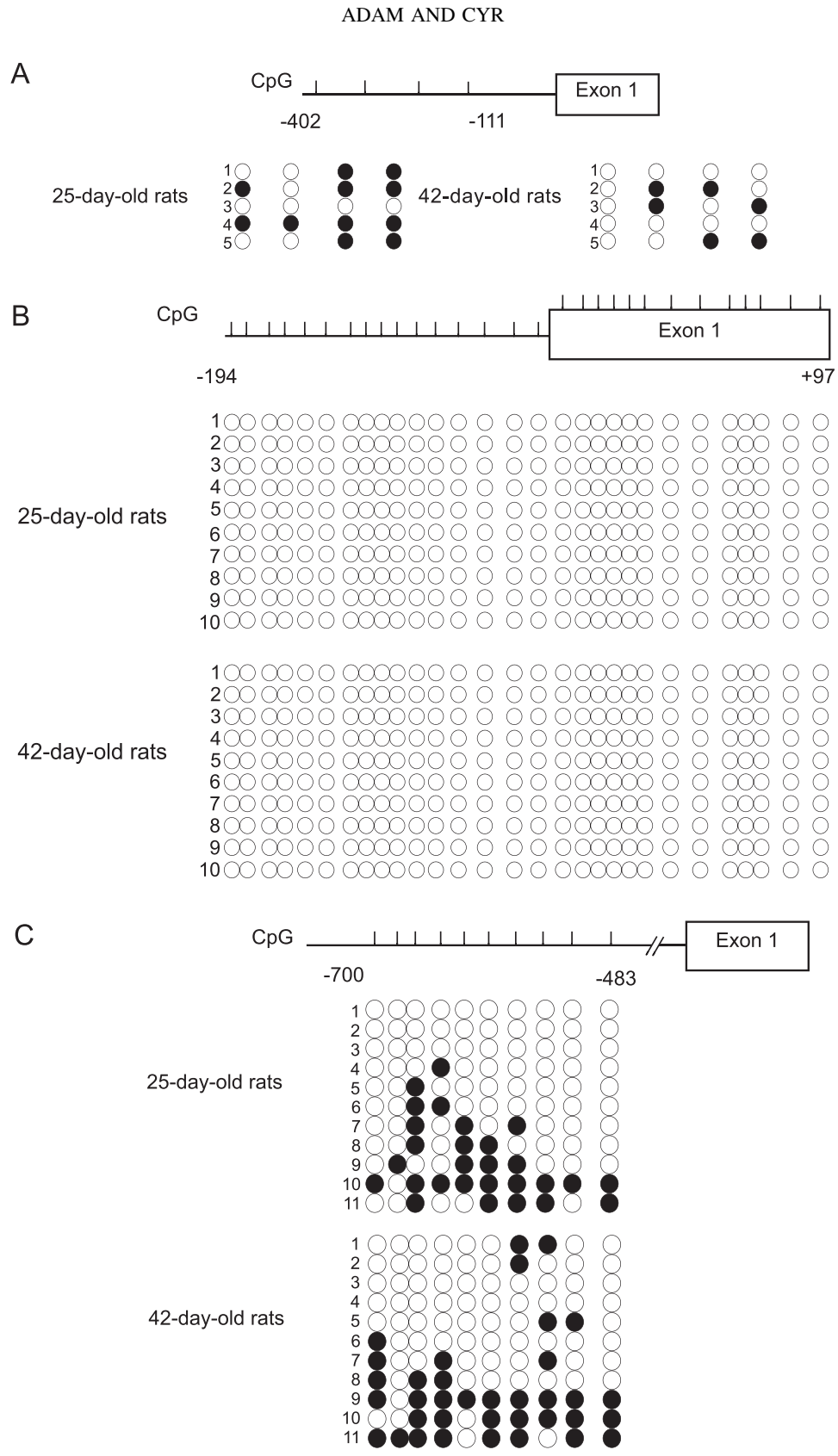
FIG. 11. DNA methylation of two regions of the *Gjb2* promoter in the epididymides of 25- and 42-day-old rats. **A**) The *Rhox5* promoter was used as a positive control for bisulfite treatment. Schematic shows 5′ upstream region of the rat *Rhox5* promoter containing 4 CpG (vertical bars). Methylation status of 5 clones of 25- and 42-day-old rats is shown. **B**) Schematic shows 5′ upstream region of rat *Gjb2* proximal promoter and part of exon 1 (−194 to +97) containing 29 CpG. The methylation status of 10 clones of 25- and 42-day-old rats were analyzed. Data show no changes in CpG methylation between the different ages for *Gjb2* promoter. **C**) Methylation analysis of region 2 of the *Gjb2* promoter in the epididymis. Schematic shows region 2 of the Cx26 promoter. Methylation status of the upstream region of the *Gjb2* promoter (−700 to −483) was assessed by bisulfite treatment on chromatin of 25- and 42-day-old rats. A total of 11 clones were sequenced and analyzed. Data show a slight increase in DNA methylation in older animals. Methylation status of each CpG is indicated by an open circle (unmethylated) or a closed circle (methylated). Base pair positions are indicated relative to the tss.
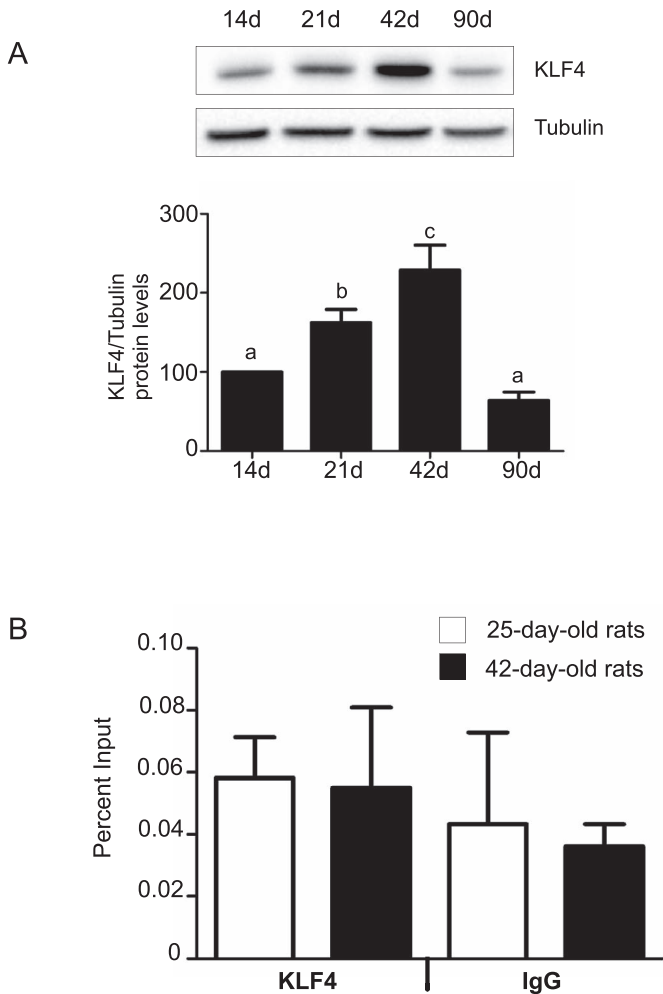
FIG. 12. KLF4 levels in the proximal epididymis during postnatal development and its recruitment to the *Gjb2* promoter. **A**) Western blot analysis of KLF4 during postnatal epididymal development (upper panel). Data indicate KLF4 protein levels increased during epididymal development until day 42 but are decreased in 90-day-old rats. Data are mean ± SEM; n = 4 proximal epididymides per age. **B**) ChIP was performed using chromatin from the proximal epididymal region of 25- and 42-day-old rats. qPCR was used for quantification. Results show that KLF4 does not interact with the *Gjb2* promoter in vivo at either age and that these are not different from IgG samples. Statistical analysis was done using one-way analysis of variance (ANOVA) followed by a Newman-Keuls test. Data are mean ± SEM; n = 4 separate experiments. Different letters indicate significant differences ($P < 0.05$).

various cancer cells [37, 38]. In the epididymis, there was no increased DNA methylation in older rats. A recent study of decreased expression of GJB2 in the cochlea of mimetic aging rats found no methylation on the proximal promoter of the *Gjb2* gene [68]. Interestingly, however, the authors observed hypermethylation of a different CpG island, located in a region upstream of the proximal promoter of the *Gjb2* gene. We therefore examined whether this region of the *Gjb2* promoter might be responsible for the decreased expression of *Gjb2* in the proximal epididymis. Although we observed a small increase of 8.2% in methylated CpG in this distal region of the promoter, it is unlikely that this is sufficient to explain the decreased binding of TFAP2A and SP1 to the *Gjb2* promoter. Similar results have been reported in esophageal cancer cells, where the down-regulation of *Gjb2* was not related to promoter methylation [48].

KLF4 is a known repressor of GJB2 during skin development, since in mice embryos mutated for *Klf4*, the skin barrier is impaired, due to high levels of GJB2 [16, 45]. KLF4 appeared to be a strong candidate as a repressor of *Gjb2* during the epididymal differentiation, since it is expressed in the epithelium of the epididymis. Our data show that KLF4 levels increase as a function of epididymal epithelial cell differentiation, similar to what has been reported in mice [69]. However, our results indicate that KLF4 is not recruited to the *Gjb2* promoter in the epididymis and is therefore not directly implicated in the repression of *Gjb2* expression.

This study provides new information on the transcriptional regulation of *Gjb2* in the epididymis during postnatal differentiation of the epithelium, and on mechanisms involved in its regulation. We have identified an adenine as a single transcription start site for *Gjb2* rat promoter in the epididymis. Our data show that SP1 and TFAP2A transcription factors are involved in the transcriptional activity of the *Gjb2* promoter in the epididymis. SP1 was shown to be necessary for *Gjb2* expression and while TFAP2A is recruited on the promoter of *Gjb2* in both RCE-1 cells and in the epididymis, it does not appear to be essential for the expression of the *Gjb2* gene. The recruitment of these two transcription factors on the *Gjb2* gene promoter decreases with age when *Gjb2* is no longer detectable in differentiated epitheliums. DNA methylation and KLF4 transcription factors are not involved in the decrease of GJB2 expression but may involve other transcription factors and regulatory processes.

ACKNOWLEDGMENT

REFERENCES

1. Robaire B, Hermo L. Efferent ducts, epididymis and vas deferens: structure, functions and their regulation In: Knobil E, Neill J (eds.), The Physiology of Reproduction. New York: Raven Press; 1988:999–1080.
2. Robaire B, Hinton B, Orgebin-Crist MC. The epididymis In: Knobil E, Neill J (eds.), Knobil and Neill's Physiology of Reproduction, 3rd ed. New York: Elsevier; 2006:1071–1148.
3. Hermo L, Robaire B. Epididymal cell types and their functions In: Robaire B, Hinton B (eds.), The Epididymis: From Molecules to Clinical Practice. New York: Kluwer Academic/Plenum Publishers; 2002; 81–102.
4. Hermo L, Barin K, Robaire B. Structural differentiation of the epithelial cells of the testicular excurrent duct system of rats during postnatal development. Anat Rec 1992; 233:205–228.
5. Sun EL, Flickinger CJ. Development of cell types and of regional differences in the postnatal rat epididymis. Am J Anat 1979; 154:27–55.
6. Rodriguez CM, Kirby JL, Hinton B. The development of the epididymis. In: Robaire B, Hinton B (eds.), The Epididymis: From Molecules to Clinical Practice. New York: Kluwer Academic/Plenum Publishers; 2002:351–367.
7. Agarwal A, Hoffer AP. Ultrastructural studies on the development of the blood-epididymis barrier in immature rats. J Androl 1989; 10:425–431.
8. Pelletier RM. Freeze-fracture study of cell junctions in the epididymis and vas deferens of a seasonal breeder: the mink (*Mustela vison*). Microsc Res Tech 1995; 30:37–53.
9. Guan X, Inai T, Shibata Y. Segment-specific expression of tight junction proteins, claudin-2 and -10, in the rat epididymal epithelium. Arch Histol Cytol 2005; 68:213–225.
10. Li MW, Mruk DD, Cheng CY. Gap junctions and blood-tissue barriers. Adv Exp Med Biol 2012; 763:260–280.
11. Loewenstein WR. Junctional intercellular communication: the cell-to-cell membrane channel. Physiol Rev 1981; 61:829–913.
12. Goodenough DA, Goliger JA, Paul DL. Connexins, connexons, and intercellular communication. Annu Rev Biochem 1996; 65:475–502.
13. Crespin S, Bacchetta M, Saab JB, Tantilipikorn P, Bellec J, Dudez T, Nguyen TH, Kwak BR, Lacroix JS, Huang S, Wiszniewski L, Chanson M. Cx26 regulates proliferation of repairing basal airway epithelial cells. Int J Biochem Cell Biol 2014; 52:152–160.

14. Omori Y, Yamasaki H. Gap junction proteins connexin32 and connexin43 partially acquire growth-suppressive function in HeLa cells by deletion of their C-terminal tails. Carcinogenesis 1999; 20:1913–1918.

15. Trosko JE, Chang CC, Wilson MR, Upham B, Hayashi T, Wade M. Gap junctions and the regulation of cellular functions of stem cells during development and differentiation. Methods 2000; 20:245–264.

16. Djalilian AR, McGaughey D, Patel S, Seo EY, Yang CH, Cheng J, Tomic M, Sinha S, Ishida-Yamamoto A, Segre JA. Connexin 26 regulates epidermal barrier and wound remodeling and promotes psoriasiform response. J Clin Invest 2006; 116:1243–1253.

17. Kardami E, Dang X, Iacobas DA, Nickel BE, Jeyaraman M, Srisakuldee W, Makazan J, Tanguy S, Spray DC. The role of connexins in controlling cell growth and gene expression. Prog Biophys Mol Biol 2007; 94: 245–264.

18. Friend DS, Gilula NB. Variations in tight and gap junctions in mammalian tissues. J Cell Biol 1972; 53:758–776.

19. Cyr DG. Connexins and pannexins: coordinating cellular communication in the testis and epididymis. Spermatogenesis 2011; 1:325–338.

20. Dube E, Dufresne J, Chan PTK, Cyr DG. Epidermal growth factor regulates connexin 43 in the human epididymis: role of gap junctions in azoospermia. Hum Reprod 2012; 27:2285–2296.

21. Cyr DG, Finnson KW, Dufresne J, Gregory M. Cellular interaction and the blood–epididymal barrier. In: Robaire B, Hinton B (eds.), The Epididymis: From Molecules to Clinical Practice. New York: Kluwer Academic/ Plenum Publishers; 2002:103–118.

22. Gregory M, Kahiri CN, Barr KJ, Smith CE, Hermo L, Cyr DG, Kidder GM. Male reproductive system defects and subfertility in a mutant mouse model of oculodentodigital dysplasia. Int J Androl 2011; 34:e630–641.

23. Cyr DG, Hermo L, Laird DW. Immunocytochemical localization and regulation of connexin43 in the adult rat epididymis. Endocrinology 1996; 137:1474–1484.

24. Dufresne J, Finnson KW, Gregory M, Cyr DG. Expression of multiple connexins in the rat epididymis indicates a complex regulation of gap junctional communication. Am J Physiol Cell Physiol 2003; 284:C33–43.

25. Mandon M, Hermo L, Cyr DG. Isolated rat epididymal basal cells share common properties with adult stem cells. Biol Reprod 2015; 93:115.

26. Brissette JL, Kumar NM, Gilula NB, Hall JE, Dotto GP. Switch in gap junction protein expression is associated with selective changes in junctional permeability during keratinocyte differentiation. Proc Natl Acad Sci U S A 1994; 91:6453–6457.

27. Oyamada Y, Komatsu K, Kimura H, Mori M, Oyamada M. Differential regulation of gap junction protein (connexin) genes during cardiomyocytic differentiation of mouse embryonic stem cells in vitro. Exp Cell Res 1996; 229:318–326.

28. Locke D, Perusinghe N, Newman T, Jayatilake H, Evans WH, Monaghan P. Developmental expression and assembly of connexins into homomeric and heteromeric gap junction hemichannels in the mouse mammary gland. J Cell Physiol 2000; 183:228–237.

29. Tu ZJ, Kiang DT. Mapping and characterization of the basal promoter of the human connexin26 gene. Biochim Biophys Acta 1998; 1443:169–181.

30. Tu ZJ, Kollander R, Kiang DT. Differential up-regulation of gap junction connexin 26 gene in mammary and uterine tissues: the role of Sp transcription factors. Mol Endocrinol 1998; 12:1931–1938.

31. Tu ZJ, Pan WH, Gong Z, Kiang DT. Involving AP-2 transcription factor in connexin 26 up-regulation during pregnancy and lactation. Mol Reprod Dev 2001; 59:17–24.

32. Kiang DT, Jin N, Tu ZJ, Lin HH. Upstream genomic sequence of the human connexin26 gene. Gene 1997; 199:165–171.

33. Hirschi KK, Xu CE, Tsukamoto T, Sager R. Gap junction genes Cx26 and Cx43 individually suppress the cancer phenotype of human mammary carcinoma cells and restore differentiation potential. Cell Growth Differ 1996; 7:861–870.

34. Mesnil M, Krutovskikh V, Piccoli C, Elfgang C, Traub O, Willecke K, Yamasaki H. Negative growth-control of Hela-cells by connexin genes— connexin species-specificity. Cancer Res 1995; 55:629–639.

35. Hellmann P, Grummer R, Schirrmacher K, Rook M, Traub O, Winterhager E. Transfection with different connexin genes alters growth and differentiation of human choriocarcinoma cells. Exp Cell Res 1999; 246:480–490.

36. Nishimura M, Saito T, Yamasaki H, Kudo R. Suppression of gap junctional intercellular communication via 5′ CpG island methylation in promoter region of E-cadherin gene in endometrial cancer cells. Carcinogenesis 2003; 24:1615–1623.

37. Chen Y, Huhn D, Knosel T, Pacyna-Gengelbach M, Deutschmann N, Petersen I. Downregulation of connexin 26 in human lung cancer is related to promoter methylation. Int J Cancer 2005; 113:14–21.

38. Shimizu K, Shimoichi Y, Hinotsume D, Itsuzaki Y, Fujii H, Honoki K, Tsujiuchi T. Reduced expression of the Connexin26 gene and its aberrant DNA methylation in rat lung adenocarcinomas induced by N-nitrosobis(2-hydroxypropyl)amine. Mol Carcino 2006; 45:710–714.

39. Tan LW, Bianco T, Dobrovic A. Variable promoter region CpG island methylation of the putative tumor suppressor gene connexin 26 in breast cancer. Carcinogenesis 2002; 23:231–236.

40. Dufresne J, St-Pierre N, Viger RS, Hermo L, Cyr DG. Characterization of a novel rat epididymal cell line to study epididymal function. Endocrinology 2005; 146:4710–4720.

41. Haring M, Offermann S, Danker T, Horst I, Peterhansel C, Stam M. Chromatin immunoprecipitation: optimization, quantitative analysis and data normalization. Plant Methods 2007; 3:11.

42. Bhardwaj A, Song HW, Beildeck M, Kerkhofs S, Castoro R, Shanker S, De Gendt K, Suzuki K, Claessens F, Issa JP, Orgebin-Crist MC, Wilkinson MF. DNA demethylation-dependent AR recruitment and GATA factors drive Rhox5 homeobox gene transcription in the epididymis. Mol Endocrinol 2012; 26:538–549.

43. Tian HP, Lun SM, Huang HJ, He R, Kong PZ, Wang QS, Li XQ, Feng YM. DNA methylation affects the SP1-regulated transcription of FOXF2 in breast cancer cells. J Biol Chem 2015; 290:19173–19183.

44. Reynard LN, Bui C, Syddall CM, Loughlin J. CpG methylation regulates allelic expression of GDF5 by modulating binding of SP1 and SP3 repressor proteins to the osteoarthritis susceptibility SNP rs143383. Hum Genet 2014; 133:1059–1073.

45. Segre JA, Bauer C, Fuchs E. Klf4 is a transcription factor required for establishing the barrier function of the skin. Nat Genet 1999; 22:356–360.

46. Gabriel HD, Jung D, Butzler C, Temme A, Traub O, Winterhager E, Willecke K. Transplacental uptake of glucose is decreased in embryonic lethal connexin26-deficient mice. J Cell Biol 1998; 140:1453–1461.

47. Nishii K, Shibata Y, Kobayashi Y. Connexin mutant embryonic stem cells and human diseases. World J Stem Cells 2014; 6:571–578.

48. Loncarek J, Yamasaki H, Levillain P, Milinkevitch S, Mesnil M. The expression of the tumor suppressor gene connexin 26 is not mediated by methylation in human esophageal cancer cells. Mol Carcinog 2003; 36: 74–81.

49. Ezumi K, Yamamoto H, Murata K, Higashiyama M, Damdinsuren B, Nakamura Y, Kyo N, Okami J, Ngan CY, Takemasa I, Ikeda M, Sekimoto M, et al. Aberrant expression of connexin 26 is associated with lung metastasis of colorectal cancer. Clin Cancer Res 2008; 14:677–684.

50. Xu J, Nicholson BJ. The role of connexins in ear and skin physiology— functional insights from disease-associated mutations. Biochim Biophys Acta 2013; 1828:167–178.

51. Han XH, Fan Y, Wei QJ, Xing GQ, Cao X. Understanding of the molecular evolution of deafness-associated pathogenic mutations of connexin 26. Genetica 2014; 142:555–562.

52. Bakirtzis G, Jamieson S, Aasen T, Bryson S, Forrow S, Tetley L, Finbow M, Greenhalgh D, Hodgins M. The effects of a mutant connexin 26 on epidermal differentiation. Cell Commun Adhes 2003; 10:359–364.

53. Langlois S, Maher AC, Manias JL, Shao Q, Kidder GM, Laird DW. Connexin levels regulate keratinocyte differentiation in the epidermis. J Biol Chem 2007; 282:30171–30180.

54. Carninci P, Sandelin A, Lenhard B, Katayama S, Shimokawa K, Ponjavic J, Semple CA, Taylor MS, Engstrom PG, Frith MC, Forrest AR, Alkema WB, et al. Genome-wide analysis of mammalian promoter architecture and evolution. Nat Genet 2006; 38:626–635.

55. Hennemann H, Kozjek G, Dahl E, Nicholson B, Willecke K. Molecular cloning of mouse connexins26 and -32: similar genomic organization but distinct promoter sequences of two gap junction genes. Eur J Cell Biol 1992; 58:81–89.

56. Lania L, Majello B, De Luca P. Transcriptional regulation by the Sp family proteins. Int J Biochem Cell Biol 1997; 29:1313–1323.

57. Eckert D, Buhl S, Weber S, Jager R, Schorle H. The AP-2 family of transcription factors. Genome Biol 2005; 6:246.

58. Li L, He S, Sun JM, Davie JR. Gene regulation by Sp1 and Sp3. Biochem Cell Biol 2004; 82:460–471.

59. Philipsen S, Suske G. A tale of three fingers: the family of mammalian Sp/ XKLF transcription factors. Nucleic Acids Res 1999; 27:2991–3000.

60. Dufresne J, Cyr DG. Activation of an SP binding site is crucial for the expression of claudin 1 in rat epididymal principal cells. Biol Reprod 2007; 76:825–832.

61. Seenundun S, Robaire B. Cloning and characterization of the 5alpha-reductase type 2 promoter in the rat epididymis. Biol Reprod 2005; 72: 851–861.

62. Schorle H, Meier P, Buchert M, Jaenisch R, Mitchell PJ. Transcription factor AP-2 essential for cranial closure and craniofacial development. Nature 1996; 381:235–238.

63. Zhang J, Hagopian-Donaldson S, Serbedzija G, Elsemore J, Plehn-

Dujowich D, McMahon AP, Flavell RA, Williams T. Neural tube, skeletal and body wall defects in mice lacking transcription factor AP-2. Nature 1996; 381:238–241.

64. Pihlajamaa P, Sahu B, Lyly L, Aittomaki V, Hautaniemi S, Janne OA. Tissue-specific pioneer factors associate with androgen receptor cistromes and transcription programs. EMBO J 2014; 33:312–326.

65. Hu S, Yao G, Guan X, Ni Z, Ma W, Wilson EM, French FS, Liu Q, Zhang Y. Research resource: Genome-wide mapping of in vivo androgen receptor binding sites in mouse epididymis. Mol Endocrinol 2010; 24: 2392–2405.

66. Wenke AK, Bosserhoff AK. Roles of AP-2 transcription factors in the regulation of cartilage and skeletal development. FEBS J 2010; 277: 894–902.

67. Hilger-Eversheim K, Moser M, Schorle H, Buettner R. Regulatory roles of AP-2 transcription factors in vertebrate development, apoptosis and cell-cycle control. Gene 2000; 260:1–12.

68. Wu X, Wang Y, Sun Y, Chen S, Zhang S, Shen L, Huang X, Lin X, Kong W. Reduced expression of connexin26 and its DNA promoter hyper-methylation in the inner ear of mimetic aging rats induced by d-galactose. Biochem Biophys Res Commun 2014; 452:340–346.

69. Godmann M, Kosan C, Behr R. Kruppel-like factor 4 is widely expressed in the mouse male and female reproductive tract and responds as an immediate early gene to activation of the protein kinase A in TM4 Sertoli cells. Reproduction 2010; 139:771–782.